Hindawi Publishing Corporation
Advances in Mechanical Engineering
Volume 2012, Article ID 181079, 6 pages
doi:10.1155/2012/181079

Research Article

Measurement and Model Validation of Nanofluid Specific Heat Capacity with Differential Scanning Calorimetry

Harry O'Hanley, Jacopo Buongiorno, Thomas McKrell, and Lin-wen Hu

Massachusetts Institute of Technology, Cambridge, MA 02139, USA

Correspondence should be addressed to Harry O'Hanley, hohanley@mit.edu

Received 16 May 2011; Accepted 14 October 2011

Academic Editor: Kambiz Vafai

Nanofluids are being considered for heat transfer applications; therefore it is important to know their thermophysical properties accurately. In this paper we focused on nanofluid specific heat capacity. Currently, there exist two models to predict a nanofluid specific heat capacity as a function of nanoparticle concentration and material. Model I is a straight volume-weighted average; Model II is based on the assumption of thermal equilibrium between the particles and the surrounding fluid. These two models give significantly different predictions for a given system. Using differential scanning calorimetry (DSC), a robust experimental methodology for measuring the heat capacity of fluids, the specific heat capacities of water-based silica, alumina, and copper oxide nanofluids were measured. Nanoparticle concentrations were varied between 5 wt% and 50 wt%. Test results were found to be in excellent agreement with Model II, while the predictions of Model I deviated very significantly from the data. Therefore, Model II is recommended for nanofluids.

1. Introduction

Nanofluids are unique fluids consisting of nanoparticles suspended in a base fluid. They are currently being considered for use by a wide range of industries from energy to manufacturing to medicine.

The ability to customize the characteristics of the nanofluids—through particle material selection—makes them attractive candidates for heat transfer applications. For example, nanofluids can be used as a medium to more effectively transfer energy captured from solar arrays or cool nuclear reactors.

Recent research has indicated that dispersions of nanoparticles in a base fluid, known as nanofluids, can increase the boiling critical heat flux and overall performance of thermal systems. Typical nanoparticle concentrations may range from 0.01 wt% to 50 wt%, and common particle materials include silica, alumina, copper oxide, zirconia, and carbon nanotubes [1–3]. Water often serves as the base fluid though other liquids such as ethylene glycol have been used [1].

As nanofluids are being considered for thermal applications, it is necessary to be able to predict their thermophysical properties accurately. Because nanofluids were initially considered for thermal conductivity enhancement, this property has been extensively studied [2–4]. However, there have been fewer examinations of nanofluid specific heat capacity [5, 6]. It is the objective of this paper to complement existing research by (i) measuring the specific heat capacity of water-based silica, alumina, and copper oxide nanofluids and (ii) comparing the predictions of two popular nanofluid specific heat capacity models to data.

2. Specific Heat Models

There are two specific heat models widely used in the nanofluid literature. Model I is similar to mixing theory for ideal gas mixtures [3]. It is a straight average relating nanofluid specific heat, $c_{p,nf}$, to basefluid specific heat, $c_{p,f}$, nanoparticle specific heat, $c_{p,n}$, and volume fraction, φ. Using

these parameters, Model I calculates the nanofluid specific heat as

$$c_{p,nf} = \varphi c_{p,n} + (1-\varphi)c_{p,f}. \quad (1)$$

While it is simple and thus commonly used, Model I has little theoretical justification in the context of nanofluids.

Model II [3, 7] is based on the assumption of thermal equilibrium between the particles and the surrounding fluid. Starting from an arbitrary mass of nanofluid m_{nf}, of volume V_{nf} and with a nanoparticle volumetric fraction φ, the nanofluid density is obviously $\rho_{nf} = m_{nf}/V_{nf} = \varphi\rho_n + (1-\varphi)\rho_f$, where the particle and fluid densities are ρ_n and ρ_f, respectively. The energy required to elevate the nanofluid mass is $\varphi V_{nf}(\rho c_p)_n + (1-\varphi)V_f(\rho c_p)_f$. Therefore, the nanofluid specific heat capacity per unit mass of nanofluid, that is, the nanofluid specific heat, is

$$c_{p,nf} = \frac{\varphi\left(\rho c_p\right)_n + (1-\varphi)\left(\rho c_p\right)_f}{\varphi\rho_n + (1-\varphi)\rho_f}. \quad (2)$$

A rigorous derivation of (2) is presented also in [8].

Predictions of nanofluid specific heat capacity were made using both models and compared to experimental measurements. Water was the base fluid of all nanofluids used in this investigation. Therefore, handbook values of temperature-dependent water specific heat and density were used in calculating theoretical nanofluid specific heat [9]. Additionally, the specific heat and density of the nanoparticles were assumed to be equal to the respective thermophysical properties of particle material in bulk form.

3. Nanofluids

The specific heat capacities of three nanofluids were analyzed: alumina-water (Nyacol AL20DW), silica-water (Ludox TMA 420859), and copper-oxide-water (Alfa Aesar 45407). Selected nanofluid properties are presented in Table 1.

The stock nanofluids were obtained from commercial vendors and diluted with deionized water to vary their concentrations. Prior to mixing, the nanofluids were manually agitated to ensure uniform dispersion. Dilution was performed by weight percent using a Mettler Toledo XS105 balance. Four unique concentrations were prepared for each nanofluid and are listed in Table 2. For each concentration, two identical samples were prepared and tested.

While nanofluids were diluted and prepared according to their weight fraction, calculations were performed using volume fraction. Using the nanoparticle volume, V_n, and the water volume, V_{H_2O}, the volume fraction can be calculated as

$$\varphi = \frac{V_n}{V_n + V_{H_2O}}. \quad (3)$$

Substituting in nanoparticle mass, m_n, and density ρ_n, and water mass, m_{H_2O}, and density, ρ_{H_2O} (3) can be rewritten as

$$\varphi = \frac{m_n/\rho_n}{m_n/\rho_n + m_{H_2O}/\rho_{H_2O}}. \quad (4)$$

Table 1: Nanofluid.

Nanofluid	Particle size (nm)	pH	Specific gravity
NYACOL AL20DW	50 nm	4.0	1.19
Ludox TMA 420859	32 nm	4.0–7.0	1.22–1.24
Alfa Aesar 45407	30 nm	4.6	1.50

Table 2: Nanofluid sample concentrations.

Nanofluid	Alumina-water	Silica-water	Copper-oxide-water
Conc. 1 (stock)	20 wt% (6.4 vol%)	34 wt% (19.0 vol%)	50 wt% (13.7 vol%)
Conc. 2	15 wt% (4.6 vol%)	25.5 wt% (13.5 vol%)	37.5 wt% (8.7 vol%)
Conc. 3	10 wt% (2.9 vol%)	15 wt% (8.5 vol%)	25 wt% (5.0 vol%)
Conc. 4	5 wt% (1.4 vol%)	8.5 wt% (4.1 vol%)	12.5 wt% (2.2 vol%)

Equation (4) can be used to determine the nanoparticle volume fraction of nanofluid concentrations created by dilution with deionized water.

4. Measurement Method

A heat-flux-type differential scanning calorimeter (TA Instruments Q2000) was used to measure the nanofluid specific heat capacities. The differential scanning calorimeter (DSC) measures the heat flux into a sample as a function of temperature during a user-prescribed heating regime. It accomplishes this by comparing the heat flux into a pan containing the sample with the heat flux into an empty pan. Hermetically sealed aluminum pans (TA Instruments) were used in the tests presented here.

The classical three-step DSC procedure was followed to measure specific heat capacity [10, 11]. Additionally, testing procedures adhered to protocols set forth in the ASTM Standard Test Method for Determining Specific Heat Capacity by Differential Scanning Calorimetry (E 1269-05).

The three-step DSC procedure begins with designing a heating regime, which should contain the temperature range of interest. Next, a measurement is taken with two empty sample pans loaded into the DSC. During this measurement, the baseline heat flux, Q_0, is obtained. The results of this measurement indicate the bias in the machine, allowing for it to be accounted for during data reduction.

The second measurement is of a reference sample, with a known specific heat, $c_{p,\mathrm{ref}}$. A pan containing the reference sample and an empty pan are loaded into the DSC. The heat flux into the reference sample, Q_{ref}, is recorded throughout the identical heating regime.

The third measurement is made on the actual sample of interest. A pan containing the sample and an empty pan are loaded into the DSC. The heat flux into the sample, Q_{sample}, is recorded during an identical heating regime as the previous two measurements. The heat flux curves from the

three measurements are used to comparatively determine the specific heat of the sample, $c_{p,\text{sample}}$, where

$$c_{p,\text{sample}} = \frac{Q_{\text{sample}} - Q_0}{Q_{\text{ref}} - Q_0} \frac{m_{\text{ref}}}{m_{\text{sample}}} c_{p,\text{ref}} \quad (5)$$

and m_{ref} and m_{sample} represent the masses of the reference and sample, respectively. Sample masses were measured using a Perkin Elmer AD6 autobalance.

In these tests, deionized water was used as the reference sample, with specific heat values obtained from Perry's Chemical Engineers Handbook [9]. The DSC heating procedure consisted of three steps:

(1) equilibrate and remain isothermal at 25°C for one minute,

(2) ramp to 75°C at 10°C/min,

(3) remain isothermal at 75°C for one minute.

Heat flux measurement was continuous from 25°C to 75°C. However, for analysis, specific heat capacities were calculated at 35°C, 45°C, and 55°C. For each sample of nanofluid concentration, three measurements were taken. These values were then averaged to yield the data points and related standard deviations presented in Figures 1, 2, 3, 4, 5, 6, 7, 8, and 9.

Prior to nanofluid measurement, this DSC methodology was validated by analyzing two pure fluids, ethylene glycol and glycerin. The results obtained from these measurements were compared against handbook values of specific heat for these liquids [12]. All experimental data are reported in Section 6.

5. Uncertainty Analysis

The measurement uncertainty for the specific heat was calculated by propagating the precision uncertainties of all individual measurements required to determine the specific heat. Equation (5) suggests there is a precision error associated with the heat flux measurements as well as the mass measurements. If all variables are assumed to be distributed normally, the overall measurement uncertainty, μ_{total}, is

$$\mu_{\text{total}} = \sqrt{\sum_{i}^{n} \left(\frac{\partial c_{p,\text{sample}}}{\partial x_i} u_i \right)^2}. \quad (6)$$

Here, x_i is the independent variable to be estimated and μ_i is the manufacturer reported precision of the measurement method. Here, (5) is substituted into (6) and the appropriate derivatives are taken to capture all measurement uncertainties. In this instance, each specific heat capacity measurement requires three heat flux measurements and two mass measurements. The associated precision uncertainties are reported in Table 3.

From this analysis, the precision uncertainty in the measurement of specific heat capacity for Model II was found to be about 0.07 (J/g-K).

Table 3: Reported measurement uncertainties.

x_i	μ_i (±)	Equipment type
Q_s	1.2 mW	TA Instruments Q2000
Q_{ref}	3.3 mW	TA Instruments Q2000
Q_0	10 μW	TA Instruments Q2000
m_{sample}	0.2 μg	Perkin Elmer AD6
m_{sample}	0.2 μg	Perkin Elmer AD6

Table 4: Propylene glycol.

Temperature (°C)	Theoretical c_p (J/g-K)	Measured c_p (J/g-K)
35	2.56	2.54 ± 0.191
45	2.62	2.64 ± 0.185
55	2.65	2.65 ± 0.185

Table 5: Glycerin.

Temperature (°C)	Theoretical c_p (J/g-K)	Measured c_p (J/g-K)
35	2.39	2.41 ± 0.008
45	2.41	2.42 ± 0.002
55	2.42	2.44 ± 0.001

6. Results and Discussion

DSC measurements of pure ethylene glycol and glycerin were in good agreement with literature values of specific heat capacity. The results of these tests, presented in Tables 4 and 5, validate the DSC methodology and machine calibration.

Figures 1, 2, 3, 4, 5, 6, 7, 8, and 9 show the nanofluids data and the curves predicted by Models I and II. As expected, as nanoparticle concentration increases, the specific heat capacity decreases. However, Model I largely underestimates the decrease, while Model II offers a much more accurate prediction of nanofluid specific heat capacity. These conclusions are consistent with the alumina nanofluid results reported in [3] and expand the validity of Model II to silica and copper oxide nanofluids. In [3], the researchers also found there to be a sharp departure from Model I with increasing nanoparticle volume fraction.

Even for Model II, there appear to be small discrepancies between the data and predictions. These could come from errors in the listed stock nanofluid concentrations, experimental uncertainties in dilution, or inconsistencies in using the bulk material properties in the model, instead of the actual nanoparticle properties. Recent research suggests that these properties may differ if the material is in nanoparticle form versus bulk form [8]. Investigation of these effects is left for future work.

7. Conclusions

Using a heat flux differential scanning calorimeter (DSC), the specific heat capacities of water-based silica, alumina, and copper oxide nanofluids at various nanoparticle concentrations were measured. The DSC procedure was validated by measuring the specific heat capacities of pure ethylene

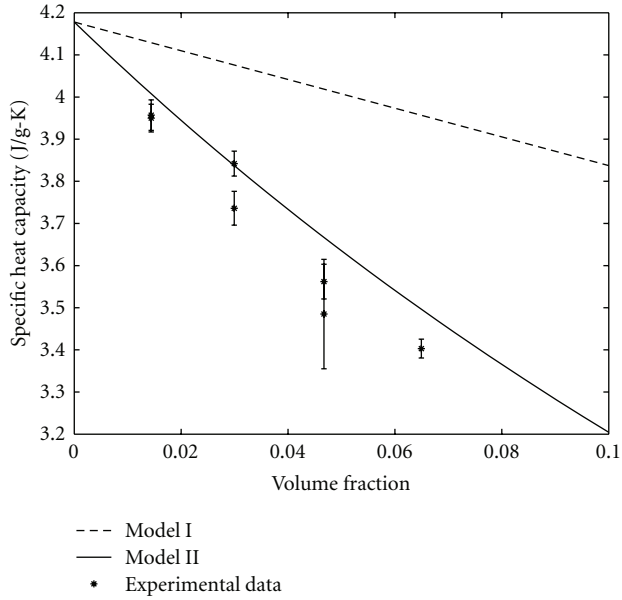

Figure 1: Alumina-water at 35°C.

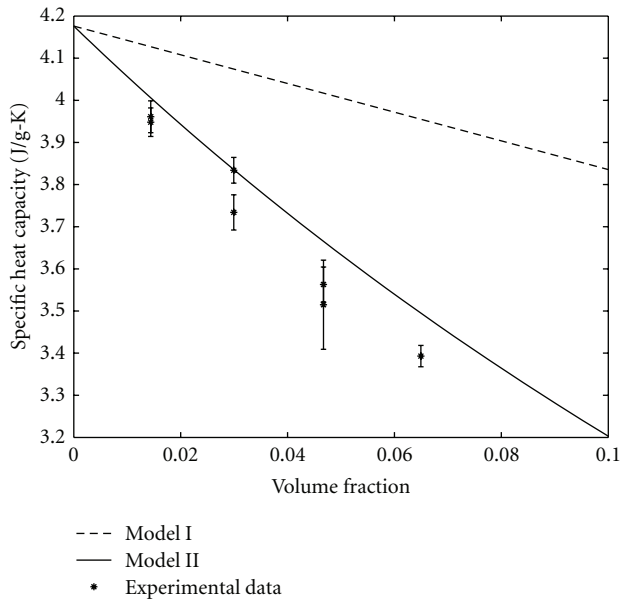

Figure 2: Alumina-water at 45°C.

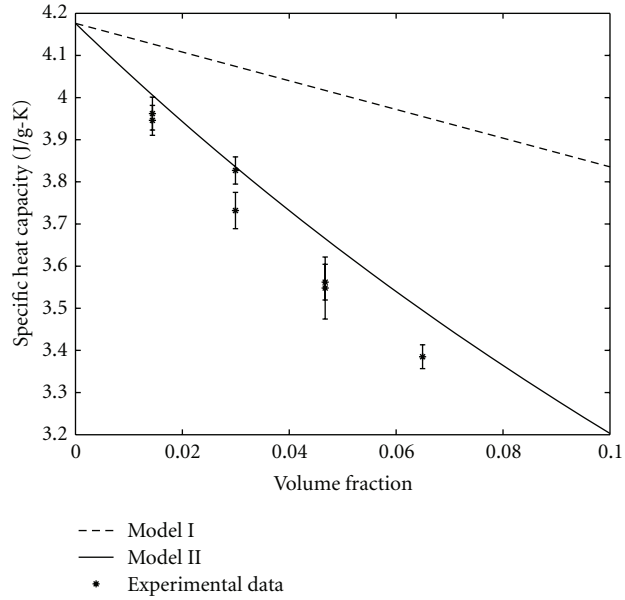

Figure 3: Alumina-water at 55°C.

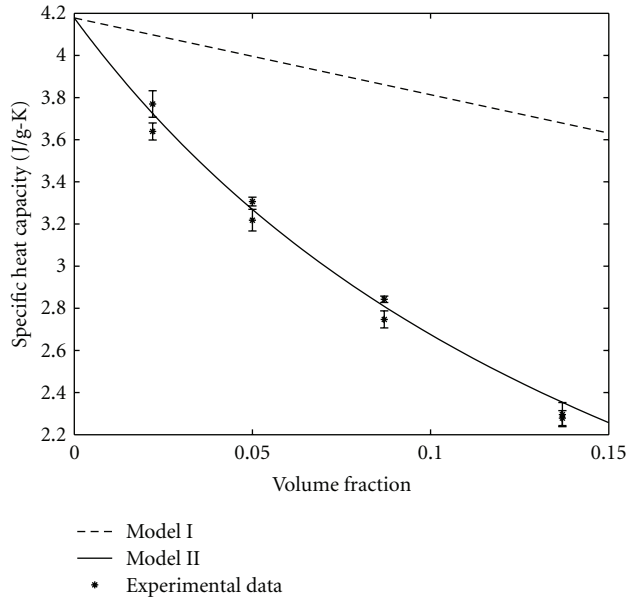

Figure 4: Copper-oxide-water at 35°C.

glycol and glycerin, which were confirmed against handbook values. The nanofluid data were used to test the predictions of two popular mixture models for specific heat. The results clearly suggest that the model based on particle/fluid thermal equilibrium (Model II) yields more accurate predictions than the model based on a straight volume-weighted average of the particle and fluid specific heats (Model I). Given its sound theoretical basis, we believeModel II is generally applicable, while Model I should be abandoned. To further improve the accuracy of Model II, future investigations could focus on measuring the actual density and specific heat of the nanoparticles in dispersion and compare them to those of the bulk materials. Additionally, future research to correlate specific heat capacity with agglomeration and sedimentation would be particularly beneficial, as such phenomena are typically unavoidable in certain applications.

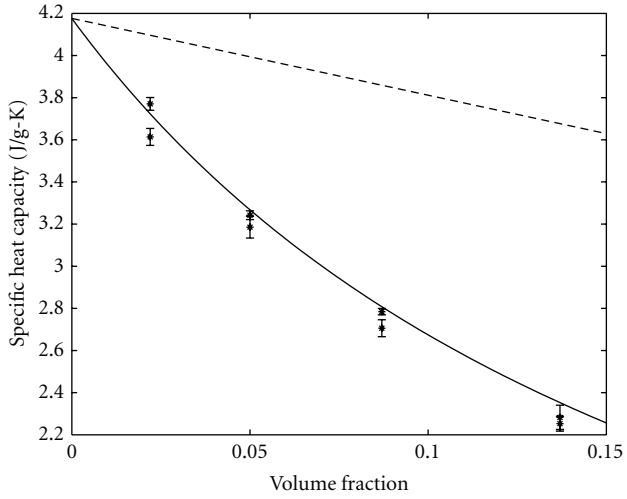

Figure 5: Copper-oxide-water at 45°C.

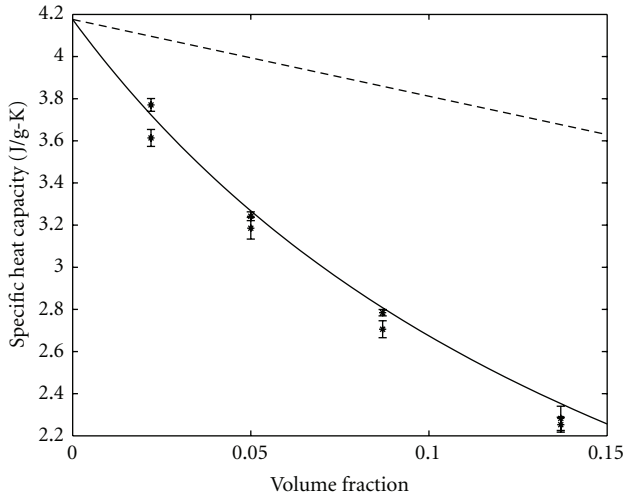

Figure 6: Copper-oxide-water at 55°C.

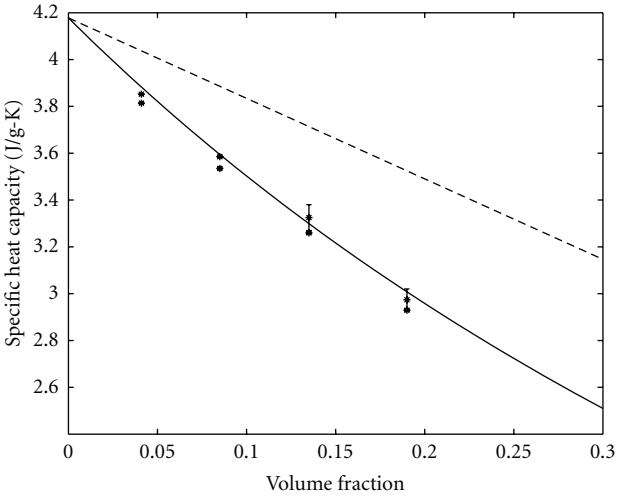

Figure 7: Silica-water at 35°C.

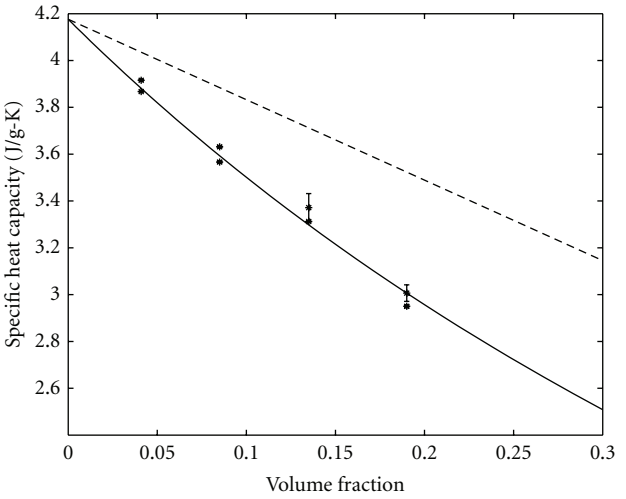

Figure 8: Silica-water at 45°C.

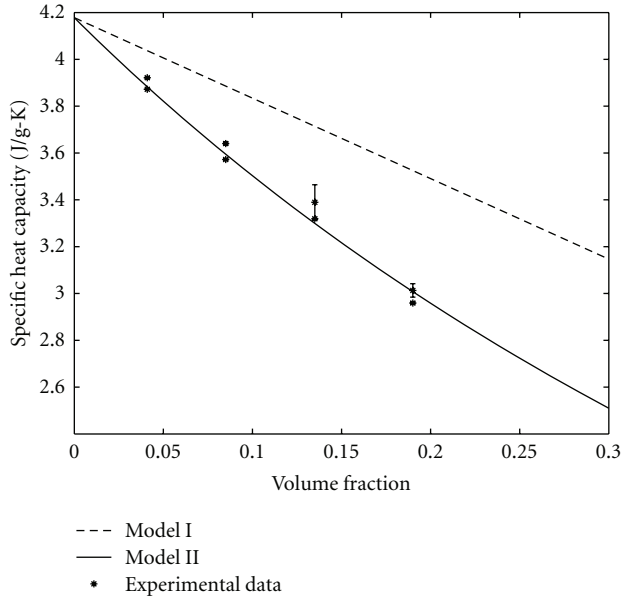

Figure 9: Silica-water at 55°C.

Nomenclature

$c_{p,f}$: Specific heat capacity of base fluid (J/g-K)
$c_{p,nf}$: Specific heat capacity of nanofluid (J/g-K)
$c_{p,n}$: Specific heat capacity of nanoparticle (J/g-K)
$c_{p,\text{ref}}$: Specific heat capacity of reference (J/g-K)
$c_{p,\text{sample}}$: Specific heat capacity of sample (J/g-K)
m_{nf}: Mass of nanofluid (g)
m_n: Mass of nanoparticles (g)
m_{H_2O}: Mass of water (g)
m_{ref}: Mass of reference (g)
m_{sample}: Mass of sample (g)
Q_{ref}: Heat flux into reference (Watts)
Q_{sample}: Heat flux into sample (Watts)
Q_0: Heat flux baseline (Watts)
Φ: Volume fraction (unitless)
ρ_f: Density of basefluid (g/cm^3)
ρ_n: Density of nanoparticles (g/cm^3)
ρ_{H_2O}: Density of water (g/cm^3)
V_{nf}: Volume of nanofluid (cm^3)
V_n: Volume of nanoparticles (cm^3)
V_{H_2O}: Volume of water (cm^3).

Acknowledgments

The Materials Research Science and Engineering Center at Harvard University offered their DSC for use in this paper. Within this facility, Dr. Philseok Kim, Dr. Kosta Ladavac, and Roxanne Kimo offered invaluable instruction and advice on the machine operation.

References

[1] K. Kwak and C. Kim, "Viscosity and thermal conductivity of copper oxide nanofluid dispersed in ethylene glycol," *Korea Australia Rheology Journal*, vol. 17, no. 2, pp. 35–40, 2005.

[2] J. Buongiorno, D. C. Venerus, N. Prabhat et al., "A benchmark study on the thermal conductivity of nanofluids," *Journal of Applied Physics*, vol. 106, no. 9, Article ID 094312, 2009.

[3] S. Q. Zhou and R. Ni, "Measurement of the specific heat capacity of water-based Al_2O_3 nanofluid," *Applied Physics Letters*, vol. 92, no. 9, Article ID 093123, 2008.

[4] S. Sinha, S. Barjami, G. Iannacchione, and S. Sinha, "Thermal properties of carbon nanotube based fluids," in *Proceedings of the Memphis-Area Engineering and Sciences Conference*, 2004.

[5] Q. He, W. Tong, and Y. Liu, "Measurement of specific heat of TiO_2-$BaCl_2$-H_2O nano-fluids with DSC," *Air Conditioning & Refrigeration*, vol. 7, no. 5, pp. 19–22, 2007 (Chinese).

[6] X. Peng, X. Yu, and F. Yu, "Experiment study on the specific heat of nanofluids," *Journal of Materials Science & Engineering*, vol. 25, no. 5, pp. 719–722, 2007 (Chinese).

[7] J. Buongiorno, "Convective transport in nanofluids," *Journal of Heat Transfer*, vol. 128, no. 3, pp. 240–250, 2006.

[8] L. P. Zhou, B. X. Wang, X. F. Peng, X. Z. Du, and Y. P. Yang, "On the specific heat capacity of CuO nanofluid," *Advances in Mechanical Engineering*, vol. 2010, Article ID 172085, 4 pages, 2010.

[9] D. Green and R. Perry, *Perry's Chemical Engineers' Handbook*, McGraw-Hill, New York, NY, USA, 8th edition, 2008.

[10] G. Hohne, *Differential Scanning Calorimetry*, Springer, New York, NY, USA, 2003.

[11] U.S. Department of Defense, *Military Handbook—MIL-HDBK-17-3F: Composite Materials Handbook, Volume 3—Polymer Matrix Composites Materials Usage, Design, and Analysis* , U.S. Department of Defense.

[12] C. Yaws, *Chemical Properties Handbook*, McGraw-Hill, New York, NY, USA, 1999.